Geo-Marine Letters (1992) 12:150–156

Geo-Marine Letters

Geotechnical Properties and Preliminary Assessment of Sediment Stability on the Continental Slope of the Northwestern Alboran Sea

J. Baraza,[1] G. Ercilla,[1] and H. J. Lee[2]

[1]Instituto Ciencias del Mar CSIC, Paseo Nacional s/n, 08039 Barcelona, Spain, and [2]U.S. Geological Survey, 345 Middlefield Road, Menlo Park, CA 94025, USA

Manuscript received 26 June 1991; revision received 12 December 1991

Abstract. Laboratory analysis of core samples from the western Alboran Sea slope reveal a large variability in texture and geotechnical properties. Stability analysis suggests that the sediment is stable under static gravitational loading but potentially unstable under seismic loading. Slope failures may occur if horizontal ground accelerations greater than 0.16 *g* are seismically induced. The Alboran Sea is an active region, on which earthquakes inducing accelerations big enough to exceed the shear strength of the soft soil may occur. Test results contrast with the apparent stability deduced from seismic profiles.

Introduction

There is ample historical and geologic evidence that earthquake-generated slope instability is common in the marine environment (Field and others 1982; Lee 1989). Stability analyses indicate that seismic shaking contributes to triggering of submarine landslides and failures in sedimentary deposits in many seismically active regions, including the Mediterranean (El-Robrini and others 1985; Perissoratis and others 1984). Earthquake-generated submarine mass flows may also constitute important mechanisms of downslope sediment transport (Morgenstern 1967; Saxow and Nieuwenhuis 1982). The ignorance of the geotechnical properties of marine sediment and their response to seismic disturbance is a serious impediment for the knowledge of the stability of seafloor areas subjected to earthquakes. The present paper summarizes the results of geotechnical tests performed on samples from the northwestern Alboran Sea, a seismically-active area in the southwestern Mediterranean. The purpose is to estimate the stability of the near-surface slope sediments, especially with respect to earthquake loading.

The physiography of the area is reported on by Ercilla and others (1992). The western Alboran Sea consists of a smoothly inclined margin with low slope gradients. Average gradients range from 0.3 to 0.8° on the eastern and western sectors, and are steeper (0.4 to 2.7°) on the central sector, with locally higher gradients (up to 9°) on canyon walls and floors. The base-of-slope gradients are lower than 0.2° (Ercilla and others 1992). The Quaternary sediments reach their maximum thickness (>200 m) on the lower slope and within the basin. On seismic profiles (Fig. 1), Pliocene and Quaternary sequences consist of basinward-thickening units formed by alternating, continuous, and discontinuous stratified reflectors. There is no evidence of large-scale instability features, such are slides or slumps, in the recent sediments. According to Ercilla and others (1992) some relatively small (3–4 km long, 20–40 m thick) debris flow deposits appear deeper in the sediment column, but are practically absent toward the top of the Quaternary sequence. Debris flow deposits presently occur on the seafloor near the levees of one active channel in the western sector. The relative decrease in number of instability-related features indicates that increasing sedimentary stability prevailed during the upper Quaternary.

Methods

Nine 7.5-cm-diameter, 5-m-long gravity cores were taken for geotechnical purposes (Fig. 2) in water depths between 95 and 670 m. An advanced geotechnical testing program provided maximum geotechnical information from the retrieved cores. The testing program included measuring of index properties, vane shear strength tests, constant rate of strain (CRS) consolidation tests, and static triaxial tests with pore pressure measurements (for detailed procedures see Lee 1986; Baraza and others 1990 and references therein). Test results allow us to estimate the sediment shear resistance and the maximum static or earthquake-induced shear stresses to which the sediment can be subjected without developing failure.

Results

Sediments

Cores were retrieved within three approximately north–south sampling transects (Fig. 2). On the eastern transect, a

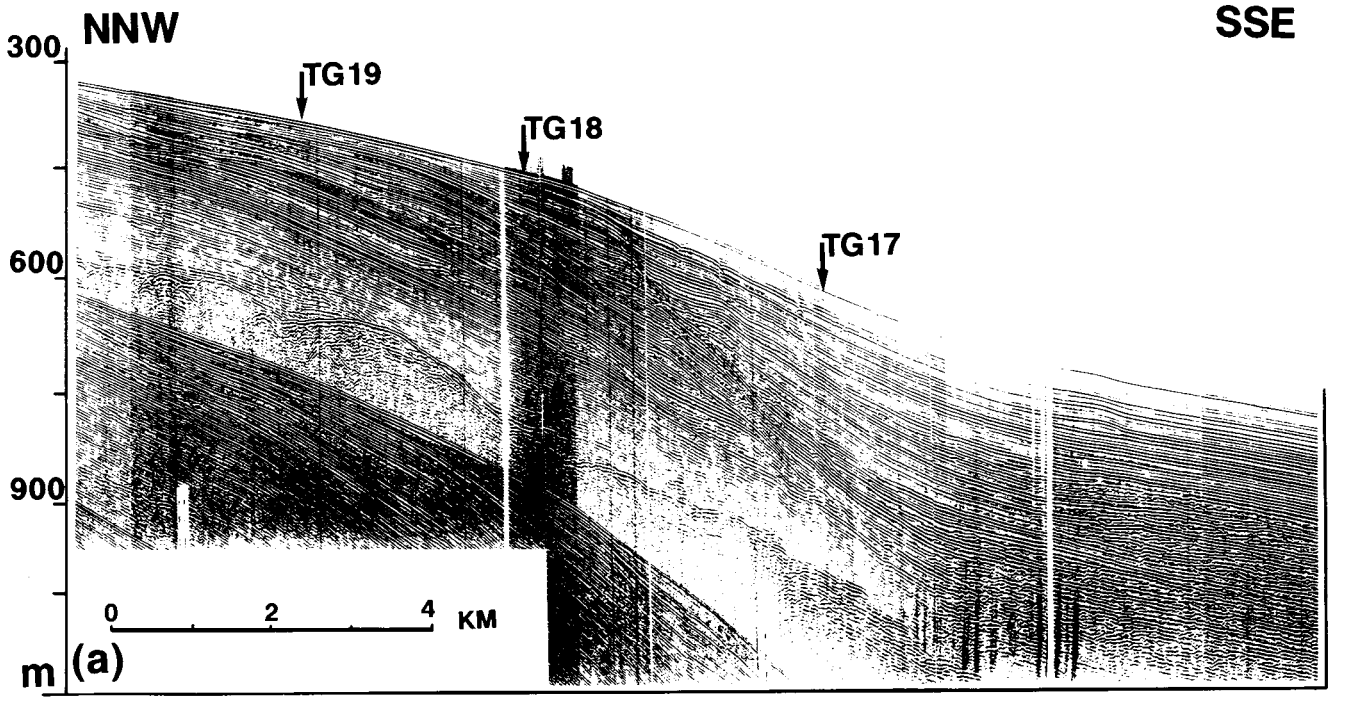

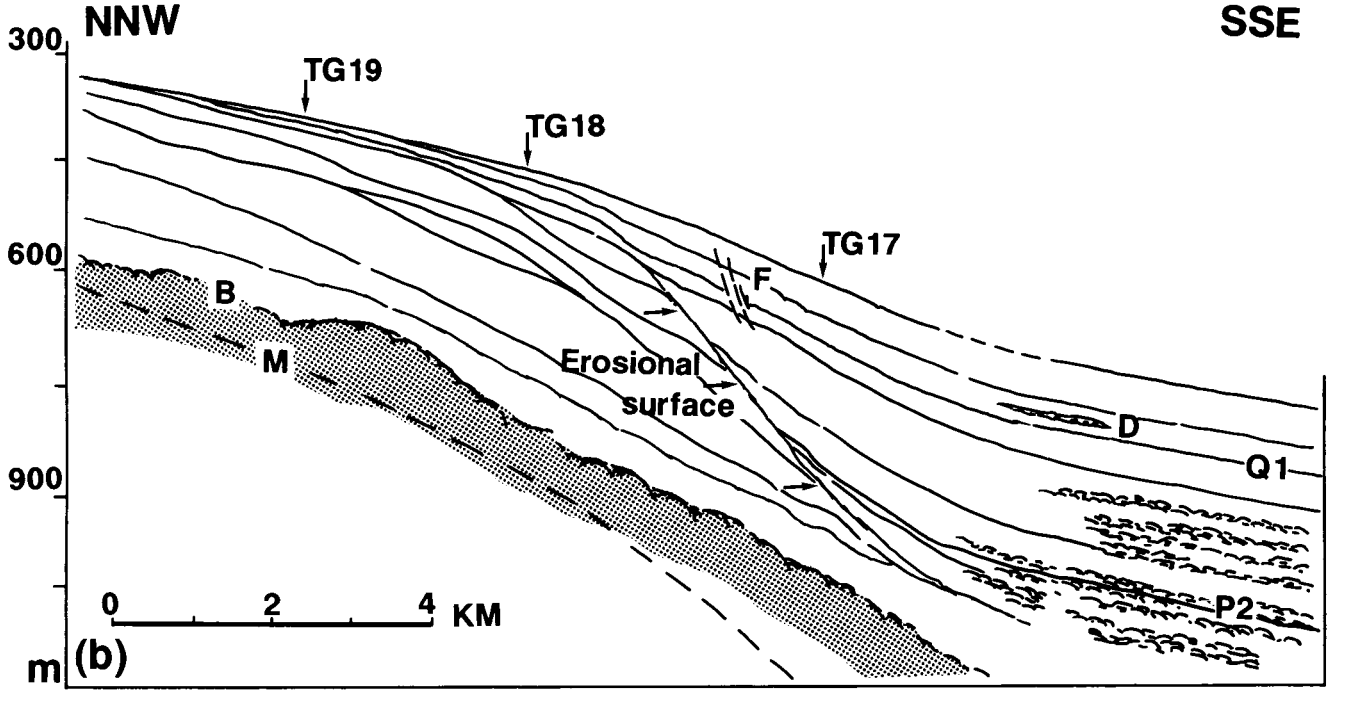

Figure 1. Airgun (10 in^3) seismic line 105 (a) and interpretative drawing (b) (location see Fig. 2). Thickening offshore, Quaternary sedimentary wedges develop onlapping a Pliocene erosive surface (marked by arrows). Intercalated, continuous, parallel, and chaotic reflectors characterize the lower Quaternary sequence on the middle slope, whereas continuous parallel or semi-transparent acoustic facies occur within the upper Quaternary sequence. Note the practically total absence of instability-related features within the upper Quaternary sequence. Only two small faults (F), and a thin debris flow deposit (D) appear. Legend: Q1 and P2 correspond to the top of the lower Quaternary and the top of the Pliocene, respectively, as interpreted by Ercilla and others (1992). B, acoustic basement; M, multiple.

short-length core (TG 10, 17 cm) from the outer shelf consists of sand- and gravel-sized shelly debris within a gray silty-clay matrix. On the upper slope, core TG 12 (147 cm) consists of olive gray, massive sandy clay, overlying a sequence of interbedded clayey silts and sands with dispersed, gravel-sized, shelly debris and some thin layers of gray silty mud. On the central and western transects, cores TG 17 (202 cm), 18 (185 cm), 25 (237 cm), and 26 (224 cm) consist of

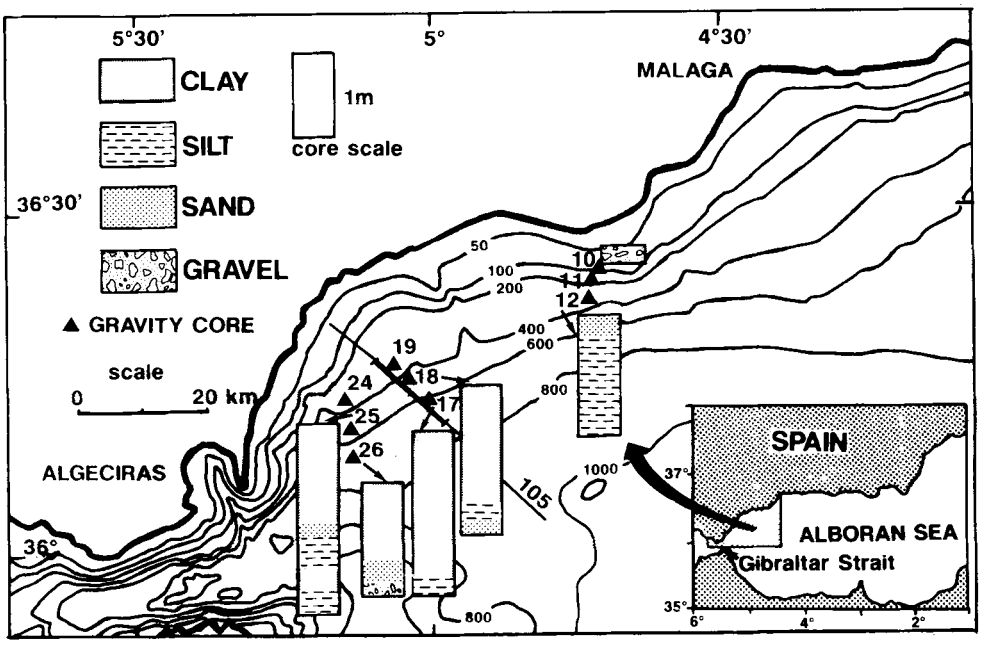

Figure 2. Bathymetric map of the study area (contours in m), with locations of coring stations, logs of recovered cores, and location of seismic line 105 (see Fig. 1).

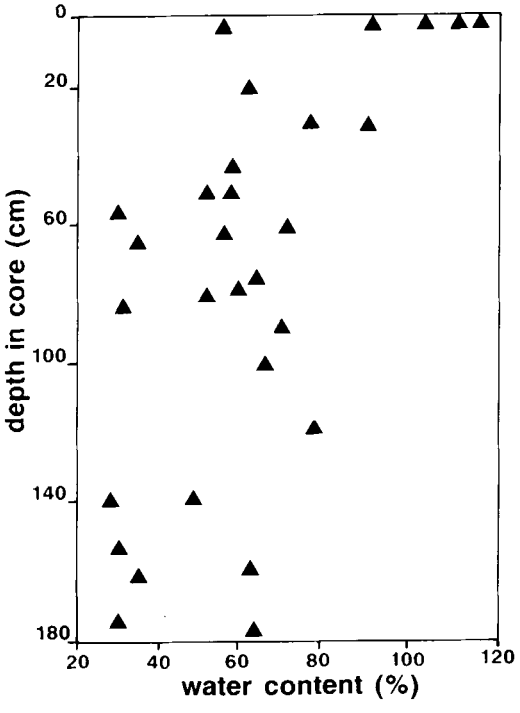

Figure 3. Water content (%) compared with depth in cores.

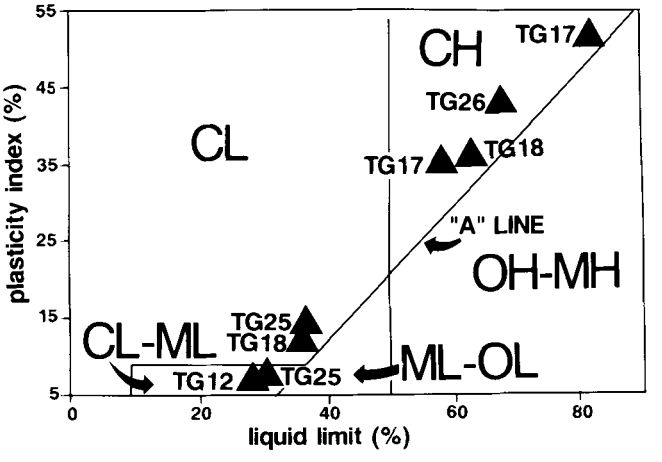

Figure 4. Plasticity chart showing engineering sediment classification according to Atterberg limits. The "A" line and the vertical and horizontal lines separate the chart into zones corresponding to different engineering classifications (CL, inorganic clay of low to medium plasticity; CH, inorganic clay of high plasticity; ML, inorganic silt of low plasticity; MH, inorganic silt of high plasticity).

greenish brown mud overlying a coarser sequence made up of interbedded sands, silts, and clays. Gravels were found at the base of core TG 26, close to the currently active Guadiaro Canyon (Ercilla and others 1992).

Index Properties

Sediment water content, wc, (Fig. 3) ranges between 52 and 117% (dry weight) for surficial sediment, decreasing down to 60–70 cm core depth, where it varies between 28 and 70%. Below this depth water content either remains constant or slightly decreases to values between 25 and 64% measured at 180 cm core depth. Atterberg limits (ASTM 1982) have been used to classify the sediment by its plasticity. Variations in wc appear to be related with the nature of sediment. On the plasticity chart (Fig. 4), all the samples plot parallel to the "A" line, but they appear within three different sectors, according to their grain size. Most of the clay samples fall within the CH sector (high plasticity, liquid limit >50% and plasticity index between 35 and 55%). Silt and silty clay samples fall within the CL and CL–ML sectors (moderate and low plasticity, respectively). Differences in plasticity are due to, among other things, different sediment texture, which will also influence other geotechnical properties (Chassefière and Monaco 1987, 1989).

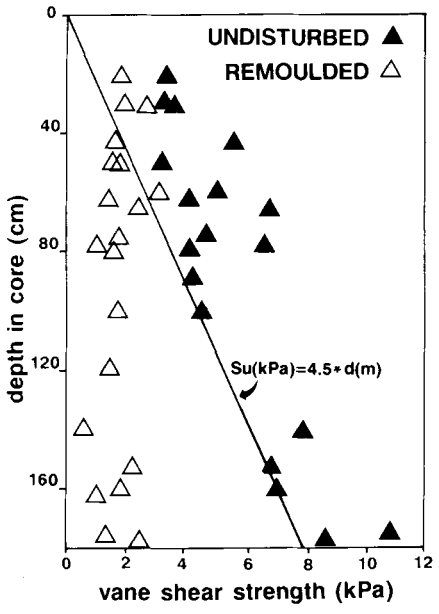

Figure 5. Undisturbed and remolded vane shear strength compared with depth in cores. A lower bound line has been drawn for the undisturbed strength (Su).

Vane Shear Strength

Vane shear strength tests were run with a 1.48 × 1.48 cm, four blade vane, at a rotation rate of approximately 90°/min. Figure 5 shows the results of undisturbed and remolded vane strength measurements versus depth in core. Undisturbed strength increases with depth, from 3 kPa at the top of the cores to 7 to 11 kPa at 160 cm. Remolded strength increases downcore from 0.5 to 3 kPa. Sensitivities range between 1.3 and 7.9 (mean = 3), corresponding to sediments of moderate to high sensitivity. On Figure 5, a line has been drawn and represents a lower bound estimate of the undisturbed shear strength. From that estimation, we will use an average strength of 4.5 kPa for analyzing the static and seismic stability of the sediment at 1 m core depth. Several testing points at 100 and 160 cm depth, passing close to this lower bound line, should correspond to the deposits most susceptible to failure. An average strength value of 35 kPa at 25 m deep into the sediment has been taken from published data from other comparable areas (Keller 1974), to get an estimation to the slope stability at depth.

Consolidation Properties

Consolidation tests (Table 1) were used to determine the sediment compressibility and to estimate the stress history of the sediment. The consolidation curve (e − log σ'_v: variation of void ratio versus log applied vertical effective stress), enables the estimation of the maximum past stress σ'_{vm} (maximum effective overburden stress to which the sediment has ever been exposed) (Casagrande 1936). Figure 6 shows the consolidation curves for two depths within core TG 12 that have different textures. Test CE305, made on the finer-grained sediment, gave a curve with a well-defined curvature point and a straight virgin segment, from which σ'_{vm} can be easily calculated. In contrast, test CE297, made on silty sediment, plot as a consolidation curve without a well-defined change in slope or a straight virgin compression segment, from which it is impossible to calculate an accurate σ'_{vm}. Poor consolidation curves may also indicate sediment disturbance, but little evidence of such disturbance (e.g. deformed lamination or other sedimentary structures) has been observed on the split cores. The results of tests run on coarse-grained samples (e.g. CE297) are not conclusive. Values of σ'_{vm} between 8 and 60 kPa have been obtained from consolidation tests; values greater than 40 kPa corresponding to poor consolidation curves are disregarded.

The overconsolidation ratio, OCR (ratio of the maximum past stress to the present overburden effective stress), ranges from 1 to approximately 5 (Table 1), corresponding to normally consolidated to slightly overconsolidated sediments. Overconsolidation may be real, or it may be apparent; true overconsolidation may indicate that part of the overlying sediment has been removed through erosion or slope failure. Apparent overconsolidation is a surficial effect that may be caused by, among other things, cementation or interparticle bonding, and is lost with depth (Silva and Jordan 1984).

The coefficient of consolidation, c_v, a measure of the rate at which the sediment consolidates, varies depending on the amount of finer grained sediment (Table 1). Values of c_v are approximately an order of magnitude lower for the muddier sediment from cores TG 17, 18, and 25 ($c_v \approx 10^{-3}$ cm^2/sec) than for the silty sections from TG 12 and TG 25 ($c_v \approx 10^{-2}$ cm^2/sec). The compression index, C_c, is a measure of the compressibility of the sediment. Low compressibility ($C_c = 0.09 - 0.15$) appears in the coarse-grained core TG 12 and at some levels of TG 17, 18, and 25. Intermediate to high compressibility ($C_c = 0.32 - 0.57$) appears in the fine grained cores TG 17, 18, 25, and 26 (Table 1).

Stability Analysis

Stability under Static Loading

Consolidated, undrained triaxial tests were run to measure the strength of sediment under an axial load and to obtain the Mohr-Coulomb failure envelope parameters ø′ (effective internal friction angle) and c′ (cohesion intercept), as well as the ratio of undrained shear strength to effective consolidation stress for normal consolidation ($Su/\sigma'_c = S$). The results of such tests are presented as a stress path (shear stress applied to the sample, q, versus mean effective confining stress, p′, throughout the test). Stress paths provide information about the sediment behavior during shear. Figure 7 represents the stress paths for five of the retrieved cores, consolidated to 70–90 kPa prior to shearing to compensate for the effects of sediment disturbance during coring (Lee 1986). A contractive response (stress path trending to the right) is observed for all sections of core TG 17, but for the rest of the cores silty sections show contractive behavior, whereas muddy sections from the same cores show a dilative response (stress path trending to the left) at higher levels of shear stress.

Obtained values of ø′ range from 28 to 31°, which are much higher than the maximum observed slopes (≤9°). This indicates a high degree of stability or a low probability of

Table 1. Results of C.R.S. consolidation tests*

Test	Core	Depth (cm)	wc (%)	γ' (kN/m^3)	σ'_{vo} (kPa)	σ'_{vm} (kPa)	σ'_e (kPa)	OCR	C_c	c_v (cm/sec^2)	Lithology
CE305	12	130	33.5	7.68	9.9	25	15	2.5	0.15	2.5×10^{-2}	Silty clay
CE297	12	147	32.8	8.29	12.2	>60	>48	5-8	0.09	1.5×10^{-2}	Silt
CE293	17	72	83.4	5.06	3.6	17	13.4	4.7	0.57	9.0×10^{-4}	Clay
CE302	17	159	54.9	6.66	10.6	40(?)	29.4	3.7	0.40	9.0×10^{-3}	Silty clay
CE301	18	73	74.3	5.49	4.0	8	4.0	1.9	0.46	1.0×10^{-3}	Clay
CE294	18	155	32.8	7.53	11.6	60(?)	48.4	5.2	0.10	8.0×10^{-2}	Silt
CE299	25	78	36.7	7.70	6.0	14	8	2.3	0.12	2.5×10^{-2}	Silt
CE304	25	148	38.1	7.66	11.3	12	0.7	1.0	0.17	3.0×10^{-3}	Silty clay
CE296	25	169	31.4	7.71	13.0	13	0	1.0	0.1	4.0×10^{-2}	Silt
CE298	26	51	64.8	5.74	2.9	11	8.1	3.8	0.32	7.0×10^{-3}	Sandy clay

*wc, water content; γ', submerged bulk density; σ'_{vo}, effective overburden stress; σ'_{vm}, maximum past stress; σ'_e, excess effective stress; OCR, overconsolidation ratio; C_c, compression index; c_v, coefficient of consolidation.

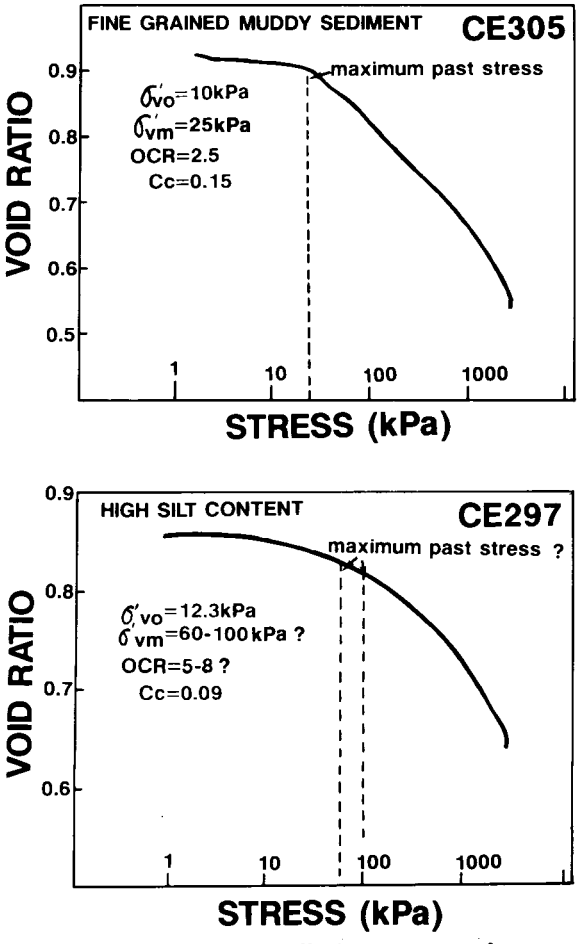

Figure 6. Void ratio versus log effective stress curves from consolidation tests on sediments of different texture from the same core (TG 12).

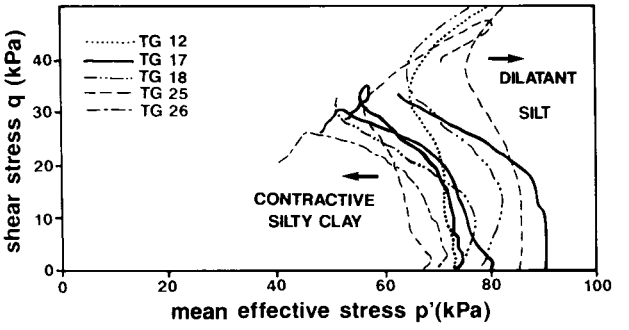

Figure 7. Stress paths corresponding to triaxial tests, with indication of contractive or dilative behavior of sediment during shear for the different cores.

drained failure under static gravitational loading. The parameter S ranges between 0.36 and 1.1, with an average of 0.49. The higher values of S correspond to dilative sediment, and suggest either interlocking particles or a bimodal fabric. In a bimodal sediment the shear planes at low confining stress pass between the coarser grains, providing little shear resistance. At greater confining pressure, the expulsion of water from within the interstitial pores causes the coarse grains to be pressed together and shear surfaces are forced to pass through the coarse grains rather than between them. This causes friction or a rapid shear strength increase with confining stress (Reimers 1982).

Stability under Seismic Loading

To produce a sediment failure during an earthquake, the cyclic shear stress must equal or exceed the shear strength of the sediment. To estimate the seismically-induced shear stress an equation from Seed and Idriss (1971) was used, modified to take into account the slope angle:

$$\tau_h = 0.65\, a_{max}\, \sigma_0\, r_d + \sigma'_0 \sin \alpha \qquad (1)$$

where τ_h is the average cyclic shear stress induced by the earthquake; σ'_0 the total and σ'_0 the effective overburden stress; a_{max} the maximum horizontal ground acceleration exerted by the earthquake; r_d, a stress reduction term that varies with depth ($r_d \approx 1$ for 1 m depth, and ≈ 0.6 at 25 m depth); and α, the slope angle. Setting $\tau_h = 4.5$ kPa, $\sigma_0 = 17$ kPa and $\sigma'_0 = 6.8$ kPa at 1 m core depth, the obtained acceleration, a_{max}, (Table 2) ranges from 0.36 to 0.43 *g*, with a mean of 0.39 *g*, for an average 2° slope. This value is an estimate of the maximum equivalent seismically-induced acceleration that the sediment may experience without developing a slope failure at 1 m below the seafloor. Using the same formula, the critical acceleration for a potential failure plane at 25 m depth in the sediment has also been estimated for each core (Table 2). Acceleration values obtained range from 0.16 *g* to 0.19 *g* (mean = 0.17 *g*). Such values imply that the slope sediment is likely to be unstable

Table 2. Calculated accelerations at 1 m and 25 m depth using Equation (1)*

Core	S	wc (%)	σ'_e (kPa)	γ' (kN/m^3)	γ (kN/m^3)	σ'_1 (kPa)	σ'_{25} (kPa)	a_{max1} (g)	a_{max25} (g)
12	0.46	33.1	21.0	18.0	7.9	18	200	0.36	0.16
17	0.41	69.1	21.4	15.9	5.8	5.8	146	0.41	0.19
18	0.57	53.5	10.0	16.5	6.5	6.5	163	0.39	0.18
25	0.60	35.4	2.9	17.7	7.7	7.7	192	0.36	0.16
26	0.36	64.8	8.1	15.8	5.7	5.7	143	0.43	0.19

*S, strength parameter: S_u/σ'_c; wc, water content; σ'_e, excess effective stress; γ' and γ, submerged and bulk density of the sediment, respectively; σ'_1 and σ'_{25}, effective overburden stress at 1 and 25 m core depth, respectively; a_{max1} and a_{max25} critical acceleration S at 1 and 25 m below seafloor, respectively.

at depth under much lower levels of earthquake-induced acceleration than near the surface. Accelerations somewhat above the critical value, however, may be experienced by many slopes without developing overt indications of failure (Lee and Edwards 1986).

Two approaches were used to estimate the seismic stability of the western Alboran Sea slope, with the presently available data.

The first approach is to evaluate the slope stability empirically by comparison with data from other comparable areas. Baraza and others (1990) reported critical horizontal accelerations for normally consolidated sediments of the Ebro margin slope northwestern Mediterranean) between 0.18 and 0.30 g for a level seafloor, and 0.09 to 0.17 g for a 10° slope. Lee and Edwards (1986) obtained values of 0.13 g or higher, corresponding to apparently stable slopes in areas of high seismicity in Alaska and California. The calculated average values of the critical acceleration (0.17 to 0.39 g) for the western Alboran Sea sediment are up to three times higher than the values obtained in Alaska and California margins, but comparable with those of stable slopes in the western Mediterranean.

A second approach is to estimate the magnitude of an earthquake that could induce an acceleration on the seafloor large enough to produce a failure, and to determine whether such an earthquake is likely to occur near the study area. Figure 8 shows the epicenters of the largest earthquakes historically recorded and areas with a greater density of shocks (Sanz de Galdeano and López Casado 1988). Although a typical earthquake within the study area has a magnitude ≤4, a 7.2 magnitude event occurred northwest of Motril in 1954 (Hatzfeld 1976), and a 7.0 magnitude earthquake may occur offshore near the western Alboran Sea slope (Udías and others 1976).

An equation by Joyner and Boore (1981) correlates the peak horizontal acceleration induced by an earthquake with other earthquake parameters such as the magnitude and distance from the observed site to the seismic source:

$$\log A = -1.02 + 0.249\ M - \log r - 0.00255\ r + P. \quad (2)$$

We have used their approach in a general sense, by setting A equal to the peak horizontal acceleration in g, M to the earthquake magnitude, r to the horizontal distance to the epicenter, and P to zero (for 50 percentile values). Following this approach, an average distance of 13 km has been obtained at which a 7.0 magnitude earthquake may induce a horizontal ground acceleration of 0.43 g, sufficient to produce a surficial slope failure. A 7.0 magnitude earthquake

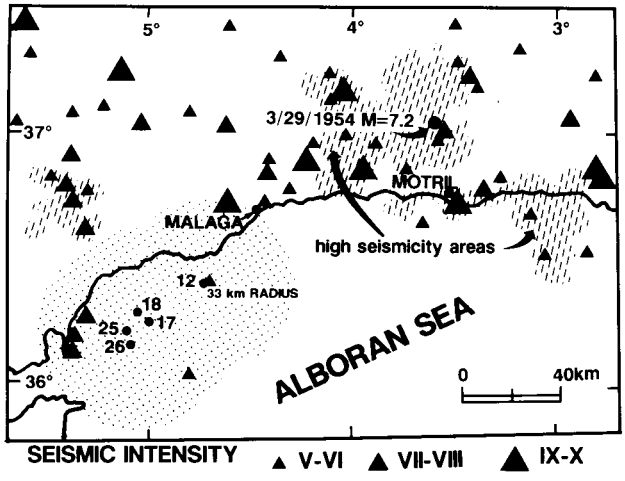

Figure 8. Map of the historically most important earthquake epicenters near the study area, and location of the maximum magnitude earthquake (7.2) recorded in recent times. Dashed areas indicate zones with a large concentration of epicenters. Stippled areas indicate zones within 33 km radius of the coring stations.

may induce a ground acceleration of 0.16 g, necessary to initiate a failure at 25 m depth, at a distance of 33 km from the seismic source. The effects of a given magnitude earthquake may be amplified by the local soil conditions, and the distance to which these acceleration values would be induced may then be higher.

No important earthquakes have been recorded with epicenters within a 13 km radius of the coring stations (Fig. 8); however, a larger number of moderate to strong earthquake epicenters are located inside the 33 km radius of the coring stations. Such regional seismicity implies that earthquakes capable of inducing ground accelerations (0.16 g) large enough to initiate a slope failure at depth have been recorded in the last fifty years. Therefore, the possibility of an earthquake capable of causing a slope failure should be considered.

Discussion and Conclusions

Stability analyses suggest that failures resulting from static, gravitational loading are unlikely on the western Alboran Sea slope, given the steep slopes necessary to start a failure if no additional, external forces are applied. Similarly, the two approaches to evaluate the stability of the western Alboran Sea slope under seismic loading indicate that a surficial sediment failure is unlikely, because of the high horizontal

ground accelerations necessary to exceed the sediment strength, except perhaps for the muddier sediment of the western and central sampling transects. However, both approaches show that instability is likely to be produced at depth in the sediment column. From a geotechnical point of view, the first approach has a greater possibility of being valid because it is based on correlations with known unstable slopes formed by sediments having similar geotechnical properties. The second approach is based only on the assumption that a given acceleration on the seafloor develops shear stresses that exceed the shear strength of the sediment. However, such a condition may probably happen only over a very short time, and the result may not be an observable landslide or slope failure, but only a limited deformation.

From the geotechnical properties and behavior of the sediment, and knowing the seismicity of the area we conclude that the western Alboran Sea slope can be characterized as potentially unstable in a general sense. Due to the relatively low seismic accelerations needed to exceed the sediment strength at depth, the likelihood of deep-seated slope failures is greater than of surficial failures. This potential instability contrasts with the practically total absence of failures in the Quaternary sequence, based on seismic records. The reason for such a contradiction between stability estimates and field observations may be that estimations have been mostly based on static strength instead of cyclic strength properties. Cyclic triaxial test results will provide a better estimate of the behavior of the sediment under seismic stresses and more accurate values of the critical horizontal acceleration for the near surface and deep sediment. Instability may have affected the most surficial sediment but observation of such instability is limited due to low resolution of the available seismic records. Another limitation of the present study is that calculations are based on very short cores (maximum length, 180 cm). Any change in sediment characteristics deeper in the sediment column (e.g. presence of weak or especially strong sediment at depth, or thick localized sand deposits that could liquify during an earthquake) should be taken into account when evaluating the stability of sediment at depth.

Acknowledgments. This paper was improved by comments from P. Cochonat, B. Chassefière, M. Hampton, and R. Kayen. W. McArthur assisted in the geotechnical testing. Support was provided by the "Alboran Sea Project" of the Spanish CICYT (Ref. GEO89-0829), and the Spanish Consortium for ODP.

References

ASTM, 1982. Annual book of ASTM Standards, Part 19, Natural Building Stones, Soil and Rock. *American Society for Testing and Materials,* Philadelphia, 710 pp.

Baraza, J., Lee, H.J., Kayen, R.E., and Hampton, M.A., 1990. Geotechnical characteristics and slope stability on the Ebro margin, western Mediterranean. *Marine Geology* **95:**379–393.

Casagrande, A., 1936. The determination of the preconsolidation load and its practical significance. *Proceedings, First International Conference on Soil Mechanics and Foundation Engineering* **3:**60–64.

Chassefière, B. and Monaco, A., 1987. Geotechnical properties and sedimentological processes of the Rhône continental margin. *Marine Geology* **74:**225–235.

Chassefière, B. and Monaco, A., 1989. Role of organic matter and particle fabric in mass-physical and geotechnical properties: Implications for drained slumping in Aegean Sea and Ionian Sea modern sediments. *Marine Geology* **87:**165–182.

El-Robrini, M., Gennesseaux, M., and Mauffret, A., 1985. Consequences of the El-Asnam earthquakes: Turbidity currents and slumps on the Algerian Margin (Western Mediterranean). *Geo-Marine Letters* **5:**171–176.

Ercilla, G., Alonso, B., and Baraza, J. 1992. Quarterly sedimentary evolution of the northwestern Alboran Sea. *Geo-Marine Letters,* **12:**144–149.

Field, M.E., Gardner, J.V., Jennings, A.E., and Edwards, B.D., 1982. Earthquake-induced sediment failures on a 0.25° slope, Klamath River delta, California. *Geology* **10:**542–546.

Hatzfeld, D., 1976. Etude de sismicité dans la région de l'Arc de Gibraltar. *Annales Géophysicae* **32:**71–85.

Joyner, W.B. and Boore, D.M., 1981. Peak horizontal acceleration and velocity from strong-motion records including records from the 1979 Imperial Valley, California, earthquake. *Bulletin of the Seismological Society of America* **71:**2011–2038.

Keller, G.H., 1974. Marine geotechnical properties: Interrelationships and relationships to depth of burial. In: Inderbitzen, A.L. (Ed.), Deep-sea sediments. Physical and mechanical properties. Marine Science Series 2, Plenum Press, New York. 77–100.

Lee, H.J., 1985. State of the art: Laboratory determination of the strength of marine soils. In: Chaney, R.C. and Demars, K.R. (Eds.), Strength testing of marine sediments: Laboratory and in-situ measurements. *American Society for Testing and Materials, Special Technical Publication 883,* Philadelphia. 181–250.

Lee, H.J., 1989. Undersea landslides: Extent and significance in the Pacific Ocean. In: Brabb, E.E. and Harrod, B.L. (Eds)., Landslides, extent and economical significance. A.A. Balkema, Rotterdam. 367–380.

Lee, H.J. and Edwards, B.D., 1986. Regional method to assess offshore slope stability. American Society Civil Engineers, *Journal of the Geotechnical Engineering Division* **112:**489–509.

Morgenstern, N.R., 1967. Submarine slumping and the initiation of turbidity currents. In: Richards, A.F. (Ed.), Marine geotechnique. University of Illinois Press, Urbana. 189–210.

Perissoratis, C., Mitropoulos, D., and Angelopoulos, I., 1984. The role of earthquakes in inducing sediment mass movement in the Eastern Korinthiakos Gulf. An example from the February 24–March 4, 1981 activity. *Marine Geology* **55:**35–45.

Reimers, M.A., 1982. Organic matter in anoxic sediments off central Peru: Relations of porosity, microbial decomposition, and deformation. *Marine Geology* **46:**175–192.

Sanz de Galdeano, C. and López Casado, C., 1988. Fuentes sísmicas en el ámbito bético-rifeño. *Revista de Geofísica* **44:**175–198.

Saxow, S. and Nieuwenhuis, J.K. (Eds.), 1982. Marine slides and other mass movements. NATO Conference Series, Series IV, Vol. 6. Plenum Press, New York. 21–49.

Seed, H.B. and Idriss, I.M., 1971. Simplified procedure for evaluating soild liquefaction potential. American Society Civil Engineers, *Journal of the Soil Mechanics and Foundation Divission* **97,** (SM9):1249–1273.

Silva, A.J. and Jordan, S.A., 1984. Consolidation properties and stress history of some deep-sea sediments. In: Denness, B. (Ed.), Seabed mechanics. Graham and Trotman, London. 25–39.

Udías, A., López Arroyo, A., and Mezcua, J., 1976. Seismotectonics of the Azores-Alboran Region. *Tectonophysics* **31:**259–289.